

Hugo F. Azurmendi*
Manuel Martin-Pastor†
C. Allen Bush
Department of Chemistry
and Biochemistry,
University of Maryland—
Baltimore County,
Baltimore, MD 21250,
USA

Received 28 May 2001;
accepted 23 July 2001

Conformational Studies of Lewis X and Lewis A Trisaccharides Using NMR Residual Dipolar Couplings

ABSTRACT: The conformations of the histo-blood group carbohydrate antigens Lewis X (Le^x) and Lewis A (Le^a) were studied by NMR measurements of one-bond C—H residual dipolar couplings in partially oriented liquid crystal solutions. A strategy for rapid calculation of the difference between theoretical and experimental dipolar couplings of a large number of model structures generated by computer simulations was developed, resulting in an accurate model structure for the compounds. Monte Carlo simulations were used to generate models for the trisaccharides, and orientations of each model were sought that could reproduce the experimental residual dipolar coupling values. For both, Le^a and Le^x , single low energy models giving excellent agreement with experiment were found, implying a compact rigidly folded conformation for both trisaccharides. The new approach was also applied to the pentasaccharides lacto-N-fucopentaose 2 (LNF-2) and lacto-N-fucopentaose 3 (LNF-3) proving its consistency and robustness. For describing the conformation of tightly folded oligosaccharides, a definition for characterization of ring planes in pyranoside chairs is proposed and applied to the analysis of the relation between the fucose and galactose residues in the epitopes, revealing the structural similarity between them.
© 2002 John Wiley & Sons, Inc. Biopolymers 63: 89–98, 2002; DOI 10.1002/bip.10015

Keywords: Lewis epitopes; NMR; dipolar coupling; oligosaccharide conformation; liquid crystal

INTRODUCTION

The Lewis blood group determinants were first identified as genetically inherited antigens found on red blood cells and more prominently on epithelial mucins. Their biological function appears to be as receptors for various lectins—in particular, the selectins—and they have been shown to be active in the inflammatory response and as differentiation antigens.¹

The determinant Le^x is the trisaccharide Gal β (1–4)[Fuc α (1–3)]GlcNAc β -1, while the structure for the epitope Le^a is Fuc α (1–4)[Gal β (1–3)]GlcNAc β -1, where Fuc is L-fucose, Gal is D-galactose, and GlcNAc is 2-acetamido-2-deoxy-D-glucose.

Most structural characterizations of oligosaccharides in solution have been based on NMR nuclear Overhauser effects (NOEs), nonselective T_1 and scalar couplings, the interpretation of which may be

*Permanent address: Departamento de Física, Universidad Nacional del Sur, Bahía Blanca, Argentina

†Present address: NMR Department, CACTUS, USC, Santiago de Compostela, Spain

Correspondence to: C. Allen Bush; email: bush@umbc.edu

Contract grant sponsor: NIH

Contract grant number: GM-57211

Biopolymers, Vol. 63, 89–98 (2002)

© 2002 John Wiley & Sons, Inc.

imprecise.^{2–5} Difficulties can result from the flexible nature of the molecule but the small number of cross peaks in NOE and the lack of an accurate model for interpretation of the long-range coupling data are also an intrinsic limitation of these methods. These techniques usually have been complemented with computational methods such as molecular dynamics that have provided a deeper understanding of the structural and dynamic properties of these systems.⁶ Recently, the development of the residual dipolar coupling method has provided a promising new tool for obtaining longer range structural information and it is being widely applied to study carbohydrates.^{7–12} While this method is particularly well suited for the study of molecules with internal motions of the first kind having motions on a picosecond time scale within a local minimum with limited excursions of the glycosidic dihedral angles ($\pm 15^\circ$),¹³ applications for the study of flexible oligosaccharides have also been recently reported.^{9,14}

In this work we present structural elucidations in partially oriented liquid crystal solutions of the trisaccharides Le^x and Le^a β -methyl glycosides based on NMR measurements of one-bond C—H residual dipolar couplings. These compounds, along with other oligosaccharides containing the same epitopes, have been studied with the techniques enumerated above by different groups,^{2,7,8,15–17} all of which concluded that both have one principal low energy conformation characterized by stacking between the fucose and galactose rings. Nevertheless, some minor but possibly significant differences occur among the reported values for the dihedral angles. Our interest here is to establish the best experimental structures for these compounds in the liquid state and to refine a methodology for structure elucidation that allows extraction of general conclusions about structural features. Our strategy for rapid calculation of the difference between theoretical and experimental dipolar couplings for thousands of model structures was also used for reanalysis of dipolar coupling data for the milk pentasaccharides lacto-N-fucopentaose 2 and 3, which include the epitopes Le^a and Le^x , respectively, linked to $\beta(1-3)\text{Gal}\beta(1-4)\text{Glc}$.^{7,8} A tool for describing the ring planes of pyranoside chairs applied to the fucose and galactose planes of the two epitopes illustrates similarities between them.

EXPERIMENTAL

Sample preparation

A ~15% bicelle stock solution in molar ratio 3:1 of 1,2-di-O-tridecanyl-*sn*-glycero-3-phosphocholine (13:0 Diether

PC) and 1,2-di-*o*-hexyl-*sn*-glycero-3-phosphocholine (06:0 Diether PC) in D_2O was prepared. Lipids were purchased from AVANTI Polar Lipids, Inc. This is a novel bicelle with behavior similar to conventional phospholipid bicelles but with improved chemical stability. The solution was mixed with vortexing in several cycles of heating to 40°C and cooling on ice.

Le^x trisaccharide β -methyl glycoside and Le^a trisaccharide β -methyl glycoside were purchased from Toronto Research Chemicals, Inc. (TRC). Each oligosaccharide was exchanged in $^2\text{H}_2\text{O}$ and lyophilized for three cycles. A sample of ~10 mg of each was dissolved in 0.25 mL of D_2O and 0.25 mL of bicelle stock solution was added to obtain a final bicelle solution of ~7.5%. Each sample was homogenized by vortexing in several cycles of heating to 40°C and cooling on ice.

NMR Spectroscopy

NMR data were acquired on a GE-Omega PSG 500 NMR instrument and processed on a Silicon Graphics workstation using Felix 2.3 software (Biosym Technologies, San Diego, CA). Residual dipolar coupling values, $^1D_{\text{CH}}$, were measured for each sample of oligosaccharide dissolved in the bicelles from the difference in the splitting of two t_1 -coupled, gradient heteronuclear single quantum correlated spectroscopy spectra (t_1 -coupled gHSQC),¹⁸ acquired at 35 and 19°C , corresponding to oriented and isotropic phases, respectively. The ^1H and ^{13}C chemical shift assignments were taken from references 2 and 17 for Le^x and Le^a , respectively, and were very similar to those obtained for the oligosaccharides in the bicellar medium at both temperatures, indicating that there is no conformational change as a consequence of the media or the temperature. To maximize the resolution in the indirect dimension, two sets of t_1 -folded experiments were acquired following a previous scheme,⁷ one with ^{13}C carrier position in the center of the anomeric region (~95 ppm) and the other in the center of the ring region (~70 ppm). For each experiment a two-dimensional (2D) matrix of 1024×256 complex free induction decay (FID) data points was acquired with 64 scans per t_1 increment. The 2D FIDs were apodized in both dimensions with a 90° -shifted sine-bell function and zero filling to give, after Fourier transformation, a 2D spectrum of 1024×1024 real points. The column corresponding to each C—H signal was carefully phased and stored. After an inverse Hilbert transformation and a zero filling to 16K, the retransformed vector showed a digital resolution of 0.2 Hz/point. Vectors from the 35°C spectrum were compared with the corresponding vector from the 19°C spectrum, and the offset required for superposition of the multiplet components was used to calculate the sign and magnitude of $^1D_{\text{CH}}$ (see Figure 1). The estimated experimental error with this procedure for these samples was ± 0.5 Hz.

Molecular Modeling and Computation

Molecular modeling was used as a tool for analysis, principally as a source of model structures to interpret dipolar

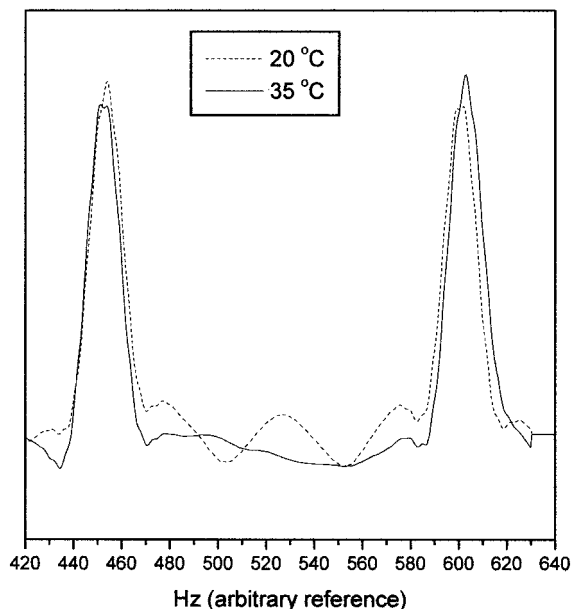


FIGURE 1 Example of slices from t_1 -coupled gHSQC, showing the difference in dipolar coupling splittings (3.3 Hz here) at 20 and 35°C in the signal of C4 of Fucose in Le^a .

couplings as is explained below. The model structures were generated using Macromodel 5.0¹⁹ in 10,000 cycles of Monte Carlo steps with force field MM3.²⁰ Better quality structures were obtained using the GB/SA continuum solvent model²¹ implemented in Macromodel mimicking water dielectric values. This protocol has been reported as a suitable one in reproducing experimental coupling constants for sialyllactones,²² and more generally for sampling carbohydrate conformations.²³

Dipolar coupling values were interpreted using the general expression and definitions^{24,25}:

$${}^1D^{CH}(\theta, \phi) = D_a^{CH} \left[(3 \cos^2\theta - 1) + \frac{3}{2} R \sin^2\theta \cos 2\phi \right] \quad (1)$$

with

$$R = D_r^{CH}/D_a^{CH}$$

$$D_a^{CH} = \frac{1}{3} [D_{zz}^{CH} - (D_{xx}^{CH} + D_{yy}^{CH})/2]$$

$$D_r^{CH} = \frac{1}{3} [D_{xx}^{CH} - D_{yy}^{CH}]$$

D_a^{CH} and D_r^{CH} are the axial and rhombic components in units of hertz of the traceless second rank diagonal tensor \mathbf{D} , with $|D_{zz}^{CH}| > |D_{yy}^{CH}| \geq |D_{xx}^{CH}|$, where R is called the rhombicity (which ranges from 0 to 2/3), and θ and ϕ are the spherical polar coordinates describing the orientation of the C—H vector with respect to the z axis of the diagonalized tensor. For the case of liquid crystal bicelle medium it can

be proved that $D_a^{CH} = -(\mu_0 h / 16\pi) S \gamma_C \gamma_H \langle r_{CH}^{-3} \rangle A_a$,^{25,26} where A_a is the unitless axial component of the molecular alignment tensor \mathbf{A} , S is the generalized order parameter for internal motions of the C—H pair,²⁷ μ_0 is the magnetic permeability of vacuum, γ_C and γ_H are the respective gyromagnetic ratios for C and H, h is Planck's constant, and r_{CH} is the distance between C and H with the angle brackets indicating vibrational average. Although both the C—H bond length and the order parameter influence the dipolar coupling, they can be folded into the magnitude of the alignment tensor as long as there are no significant differences among them.

The model structures obtained by molecular modeling are used to determine the orientation tensor. By iterative fitting, each trisaccharide model is oriented in the best way to minimize the merit function χ defined by

$$\chi = \left[\sum_1^n \frac{({}^1D_{CH}^{exp} - {}^1D_{CH}^{calc})^2}{{}^1D_{CH}^{exp})^2} \right]^{1/2} \quad (2)$$

where n is the number of C—H dipolar vectors. Experimental error is simulated by introducing variations in ${}^1D_{CH}^{exp}$, randomly selected from a Gaussian distribution whose width is adjusted through an input parameter for each iteration of the algorithm. As working hypothesis, we assume each trisaccharide to be relatively rigid having internal motion of the first kind. This assumption, which can be tested by the quality of the fit between experimental residual dipolar couplings and the values calculated from the model, justifies incorporation of any effects of a small extent of internal motion into the order parameter S . This approach requires measurement of only 5 independent vectors for the whole structure to solve Eq. (1). The assumption must be justified by the consistency of the final results and will fail in the presence of internal motions of the second kind.⁹

To find for a given model the orientation tensor that minimized the error in Eq. (2), we modified the original Powell algorithm^{7,8} based on random starting parameters values, implementing a semisystematic approach. For a given fixed model in an arbitrary coordinate frame, the Euler angles describing the orientation tensor cycled through 8 values each, for 3 values of R (0, 1/3, 2/3). The initial D_a is estimated from the maximum value of the residual dipolar couplings as $D_{CH}^{MAX}/2$.^{25,28} The algorithm discards orientations with large discrepancies (χ) between experimental and calculated dipolar couplings rapidly focusing on the better ones and using Powell optimization to obtain the lowest χ value possible. An input parameter t can be used to scale the default conditions ($t = 1$), with higher values leading to slower calculation submitting more orientations to the Powell algorithm, producing a better fit and smaller χ values. Greater values of t can be required with a larger number of dipolar couplings. All results presented here were obtained with the default value. The running time in an ordinary 500 MHz PC, with a standard linux operating system, ranges between 10 and 30 s per model structure. A flow chart and the source code of the program are available from the authors upon request.

Table I Experimental Residual Dipolar Couplings in Hz for Le^x, Le^a, and the Related Compounds LNF-2 and LNF-3 (a: Fucose; b: Galactose; c: GlcNAc)

Atom Pairs	Le ^x	Le ^a	LNF-2 ^a	LNF-3 ^a
H1—C1a	-8.6	4.3	1.8	—
H2—C2a	3.0	-1.7	-1.3	10.8
H3—C3a	3.8	-1.7	-0.8	9.3
H4—C4a	-11.0	3.3	0.3	-17.2
H5—C5a	1.5	-2.8	—	—
H1—C1b	3.7	-4.5	-5.5	—
H2—C2b	4.0	-4.0	-3.2	11.1
H3—C3b	2.0	-7.5	-4.8	10.0
H4—C4b	-3.7	6.8	5.8	-5.6
H5—C5b	3.7	-5.3	-5.8	—
H1—C1c	11.5	13.5	—	—
H2—C2c	13.7	16.3	12.1	17.2
H3—C3c	12.3	16.6	11.9	17.2
H4—C4c	11.7	16.2	10.3	15.6
H5—C5c	12.0	16.7	11.5	17.4

^a From Ref. 7.

Monte Carlo models were also constructed for the related pentasaccharides LNF-2 and LNF-3, which contain the epitopes Le^a and Le^x, respectively, for reanalysis of previously reported data.⁷ The scheme can be used to explore small parts of a larger structure, by introducing only the dipolar coupling values belonging to the region of interest, the Lewis trisaccharide epitopes in the case of these pentasaccharides.

Further analysis and graphs were done with Origin 6.0 (Microcal Software, Inc., Northampton, MA). Glycosidic dihedral angles were defined according to the IUPAC heavy-atom convention in which ϕ is defined by O₅—C₁—O₁—C_x and ψ by C_{x-1}—C_x—O₁—C₁. The glycosidic dihedral angle ϕ is not to be confused with the spherical polar coordinate angle of Eq. (1).

RESULTS AND DISCUSSION

H—C one-bond residual dipolar couplings were measured in dilute bicelle media at 7.5% concentration composed of (13:0 Diether PC / 06:0 Diether PC) 3:1, for both trisaccharides Le^x and Le^a β -methyl glycosides. Dipolar couplings were determined, for all the C—H bonds, within an estimated error of 0.5 Hz from the splittings in the ¹³C dimension of a *t*₁-coupled gHSQC experiment,¹⁸ as shown in a characteristic example in Figure 1. The experimental dipolar couplings obtained for these compounds are given in Table I and plotted in Figure 2 along with those for the related pentasaccharides LNF-2 and LNF-3.^{7,8}

Several thousands of structure models were generated using the program Macromodel¹⁹ to sample the

greatest amount of the “angular space” accessible to the molecules without bias to the possible structures by the molecular modeling. The best models could then be selected by criteria based on Monte Carlo energy minimization and χ^2 minimum value. In order to achieve this goal two different Monte Carlo protocols were used, both using the MM3 force field.²⁰ In the first method, all exocyclic dihedral angles were randomly varied over the full range, followed by 10 steps of energy minimization in vacuum. Each structure with energy less than 500 kJ above the lowest energy was kept, allowing the rapid generation of 5000 quasi-random structures out of 10,000. The second method varied only the glycosidic dihedral angles and the NAc group using 500 steps of energy minimization and the GB/SA solvent model simulation of water.²¹ We kept all the structures with energy below a threshold of 50 kJ, generating ~1500 low energy structures. Because of the limited number of significant degrees of freedom in these systems, it was found in the results to be discussed below that this lower number of structures was adequate for the dipolar coupling analysis. Likewise, other calculations have found a very limited range of low energy structures for the Lewis oligosaccharides,^{2,15,16,29–32} with minima similar to those reported here. For all the model structures the agreement with the experimental residual dipolar couplings was calculated with an estimated experimental error of 0.5Hz.

The resulting dihedral angle values were plotted in ϕ/ψ dipolar maps and the results color coded by χ and energy. The “random” model structures obtained by the first method resulted in very high values of χ (results not shown), except for a small number whose

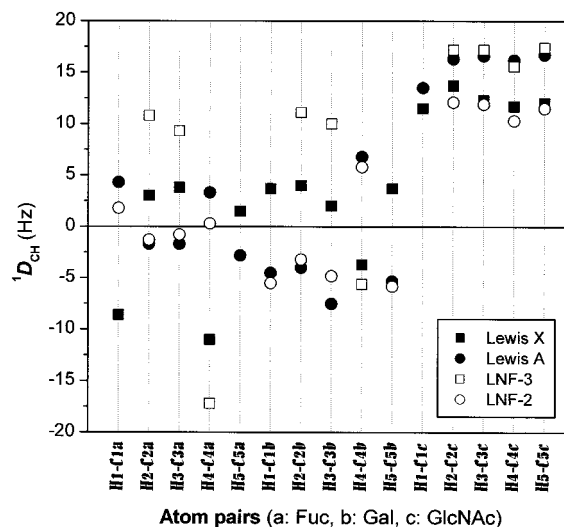


FIGURE 2 Comparison of the experimental residual dipolar couplings for Le^x, Le^a, LNF-2, and LNF-3. Data for the milk pentasaccharides taken from Ref. 7.

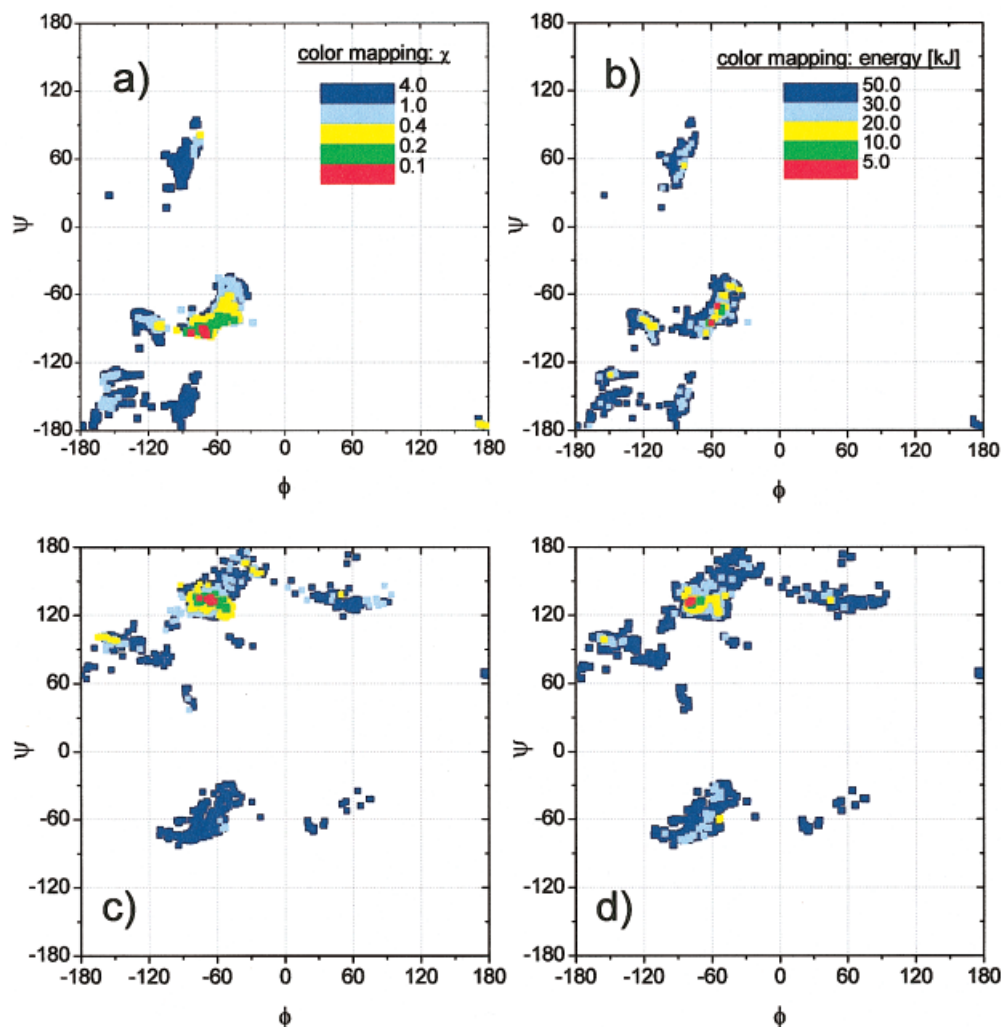


FIGURE 3 Dipolar color coded maps for Le^x . (a) and (b) Maps for linkage $Fuca(1-3)GlcNAc$ color coded by χ and relative energy, respectively. (c) and (d) Maps for linkage $Gal\beta(1-4)GlcNAc$ color coded by χ and relative energy, respectively.

dihedral angles were similar to those with low χ values in the analysis of the low energy structures from the second method shown in Figures 3 and 4. Inspection of these graphs shows a good concordance between low energy structures and those that give the lowest values of χ . The most significant differences between minimum energy conformations and those with minimum values of the error function are found for the dihedral angles ϕ in Le^x , which are about 10° for the linkage $Fuca(1-3)GlcNAc$ (-73.1° vs -63.0° for the best structures by χ and energy, respectively) and 6° for $Gal\beta(1-4)GlcNAc$ (-66.3° vs -72.6° , respectively). All other dihedral angles agree within less than 5° . The sensitivity to variations in the dihedral angles of the function χ differs for each case, because a rotation axis defining the dihedral angle parallel to the majority of the dipolar vectors affected by rotations around this axis will produce small ef-

fects on their orientations and on the error function. Inversely, the effect will be great if the rotation is around an axis perpendicular to several of the dipolar vectors. For Le^x and Le^a structures with $\chi \sim 0.1$, the glycosidic angles range between $\pm 8^\circ$ and $\pm 3^\circ$ around their minimum values. Assuming an overall error of $\pm 8^\circ$ for all the glycosidic angles and the existence of one principal conformation, the models with minimum χ reported here, on the basis of experimental parameters from liquid state, constitute a reasonable description of these molecules. Although there is an ambiguity in the correct orientation resulting from the symmetry of the dipolar interaction to a 180° rotation [Eq. (1)], the modeling is not ambiguous as only a single conformation leads to a reasonable fit to the experimental data as shown in Figures 3 and 4.

Figure 5 shows the calculated versus experimental residual dipolar couplings for the best models ob-

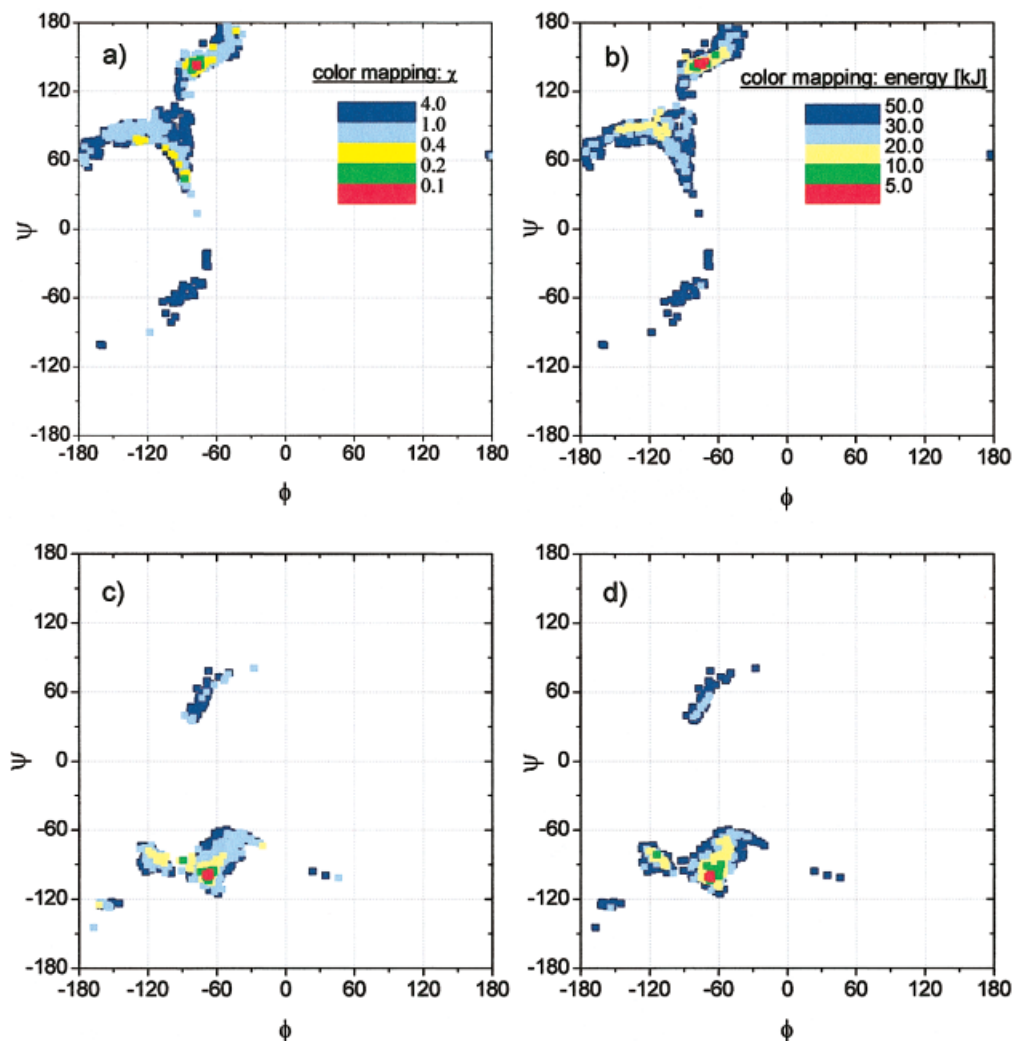


FIGURE 4 Dipolar color coded maps for Le^a . (a) and (b) Maps for linkage $\text{Fuca}(1-4)\text{GlcNAc}$ color coded by χ and relative energy, respectively. (c) and (d) are maps for linkage $\text{Gal}\beta(1-3)\text{GlcNAc}$ color coded by χ and relative energy, respectively.

tained with generally excellent agreement and no systematic deviation. The values for the glycosidic angles are summarized in Tables II and III along with previously reported values including the related compounds LNF-2 and LNF-3,⁷ for comparison. The methods used in these other studies include several computer simulations (Monte Carlo and molecular dynamics),^{2,15-17} NMR measurements^{2,7,17} and a crystal structure for Le^x with two different molecule structures in the asymmetric unit.³² Although the data indicate general agreement among the different reports, it is possible that a difference greater than 10° could be significant in the analysis of molecular interactions.

The dipolar coupling data previously reported for the compounds LNF-2 and LNF-3^{7,8} were reanalyzed with this new approach. This is an interesting test case because, although the dihedral angles reported for

LNF-2 were very similar to those obtained for Le^a , noticeable differences are observed between LNF-3 and Le^x . The results of the revised analysis agree for both Le^a and Le^x with a considerably lower values for χ than the previously reported ones (see Tables II and III). While the data of Tables II and III are based on Monte Carlo models of the full pentasaccharides, the method was also applied considering only the dipolar couplings for the rigid trisaccharide epitopes (13 for LNF-2 and 11 for LNF-3), and the results are still perfectly consistent and unambiguous on the dihedral angles, indicating the robustness of the method for use in partial structural analysis. Although these results were obtained without the use of NOEs, the solutions obtained agree well with the experimental NOE data.

To provide a more general characterization of the conformation of the Lewis epitopes, we used the large

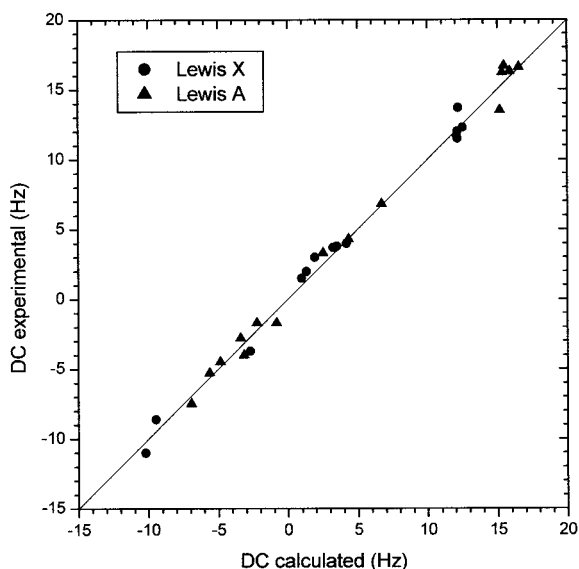


FIGURE 5 Experimental vs calculated residual dipolar couplings (DC) in Hz.

number of structures generated to analyze the relative orientations of the fucose and galactose rings. The compounds Le^x and Le^a are isomers in which the corresponding linkages of fucose and galactose to

GlcNAc are interchanged. The conventional definition of the dihedral angles ϕ and ψ do not permit a direct analysis of this important characteristic of Lewis epitopes because the relative orientation of fucose and galactose is obscured by the necessity for the four parameters to describe it. Also, the definition of the dihedral angle ψ differs for each residue in the oligosaccharides, preventing any direct comparison between them in spite of the similarity in their three-dimensional structures. Therefore a general parameter that relates these branched residues would be desirable. We propose here to define vectors perpendicular to the fucose and galactose rings by taking the cross product of the vectors between the atoms C2—C5 and O5—C3, which are embedded in an approximate plane, in such a way that

$$\mathbf{R}_1 = \mathbf{r}_{C5} - \mathbf{r}_{C2}$$

$$\mathbf{R}_2 = \mathbf{r}_{C3} - \mathbf{r}_{O5} \quad (3)$$

$$\mathbf{S} = \mathbf{R}_1 \times \mathbf{R}_2$$

Although in general \mathbf{R}_1 and \mathbf{R}_2 do not define a perfect plane, they are nearly coplanar in pyranoside chairs

Table II Glycosidic Dihedral Angles Reported for Le^x and LNF-3^a

Reference	Dihedral	Fuca(1-3)Gal	Gal β (1-4)GlcNAc	GlcNAc β (1-3)Gal	Gal β (1-4)Glc	χ
Le^x	ϕ	-73.1	-66.3			0.01
(a)	ψ	-90.5	135.0			
Le^x	ϕ	-72.5/-76.7	-80.0/-70.5			0.16/0.26
(b)	ψ	-101.2/-101	135.4/132.3			
Le^x	ϕ	-81 ± 5	-75 ± 5			0.11
(c)	ψ	-89 ± 4	136 ± 4			
LNF-3	ϕ	-40 ± 10	-65 ± 10	-95 ± 10	-69 ± 10	0.25 ^b
(d)	ψ	-90 ± 10	114 ± 10	-114 ± 10	146 ± 10	
LNF-3	ϕ	-67.6	-70.8	-73.0	-42.2	0.05 ^b
(e)	ψ	-87.4	134.6	-156.6	168.2	
LNF-3/ Le^x	ϕ	-45 ± 10	-55 ± 10			0.18
(f)	ψ	-95 ± 10	120 ± 15			
Le^x	ϕ	-59 ± 20	-61 ± 9			0.23
(g)	ψ	-88 ± 10	128 ± 7			
Le^x	ϕ	-64 ± 21	-64 ± 10			0.14
(h)	ψ	-88 ± 11	128 ± 8			
Le^x	ϕ	-45	-57			0.23
(i)	ψ	-96	122			
Le^x	ϕ	-83	-65			0.26
(j)	ψ	-97	132			
$Le^x\beta$ (1-3)Gal	ϕ	-57.8	-66.2			0.18
(k)	ψ	-84.0	120.2			

^a The references and techniques used were as follows: (a) This work, $^1D_{CH}$. (b) Crystal structures³² (adopt two simultaneous conformations). (c) Molecular modeling.¹⁶ (d) $^1D_{CH}$ and NOE.⁷ (e) This work, $^1D_{CH}$. (f-j) NOE, T_1 , and molecular dynamics.² (k) Rotating frame NOE, molecular dynamics.³¹

^b Includes 16 $^1D_{CH}$ from 5 residues.

Table III Glycosidic Dihedral Angles Reported for Le^a and LNF-2^a

Reference	Dihedral	Fuc α (1-4)Gal	Gal β (1-3)GlcNAc	GlcNAc β (1-3)Gal	Gal β (1-4)Glc	χ
Le ^a	ϕ	-76.9	-70.0			0.07
(a)	ψ	141.8	-98.8			
Le ^a	ϕ	-79.4	-75.4			0.20
(b)	ψ	142.3	-95.9			
LNF-2	ϕ	-63 \pm 10	-61 \pm 10	-105	-135	0.37 ^b
(c)	ψ	131 \pm 10	-101 \pm 10	-143	95	
LNF-2	ϕ	-74.5	-68.1	-81.6	-66.6	0.21 ^b
(d)	ψ	144.3	-95.2	-176.4	111.0	
LNF-2	ϕ	-70 \pm 10	-70 \pm 10			0.27
(e)	ψ	-140 \pm 10	-100 \pm 15			
Le ^a	ϕ	-77	-73			0.45
(f)	ψ	141	-106			

^a The references and techniques used were as follows: (a) This work, ¹D_{CH}. (b) Molecular modeling.¹⁶ (c) ¹D_{CH} and NOE.^{7,8} (d) This work, ¹D_{CH}. (e) NOE and T₁.³³ (f) NOE, long-range couplings, MD.¹⁷

^b Includes 20 ¹D_{CH} from residues.

and provide a general definition for sugars. This definition can be useful for the structure characterization of any polysaccharide by specifying the position and orientations of each "ring vector." Here we used it to study the relative orientations of fucose and galactose, which can characterize the overall shape of the epitope, an important characteristic in Lewis oligosaccharides in their role in cell adhesion through carbohydrate-lectin interactions. The analysis was done with plots of χ as a function of the angles formed by the planes in the two trisaccharides (Figure 6). An almost parallel orientation is found between the rings (or more precisely antiparallel, since the definition implies an orientation for the sugar planes which is opposite in this case). The very good correspondence between Le^x and Le^a reaffirms a previous suggestion² about the structural similarity between them.

A certain level of geometric similarity between the Le^x and Le^a is apparent from the dipolar coupling data illustrated in Figure 2. For the GlcNAc residue in each trisaccharide, the ¹D_{CH} values are large and positive, indicating that they are approximately parallel to the direction of the D_{zz} principal axis. For the Fuc and Gal residues, ¹D_{CH} magnitudes are smaller, with each value alternating in sign between the two trisaccharides (Figure 2). These features can be visualized in Figure 7, which represents the best geometry model for Le^a and for Le^x in orientations, which are consistent with the ¹D_{CH} data. Both trisaccharides are oriented so that C—H vectors of the GlcNAc residue (in red) are perpendicular to the plane of Figure 7. Le^x and Le^a are isomers in which the linkage positions of α Fuc and β Gal are interchanged. The geometric similarity is evident from Figure 7 by rotating the GlcNAc residue by $\sim 180^\circ$ about the axis represented by

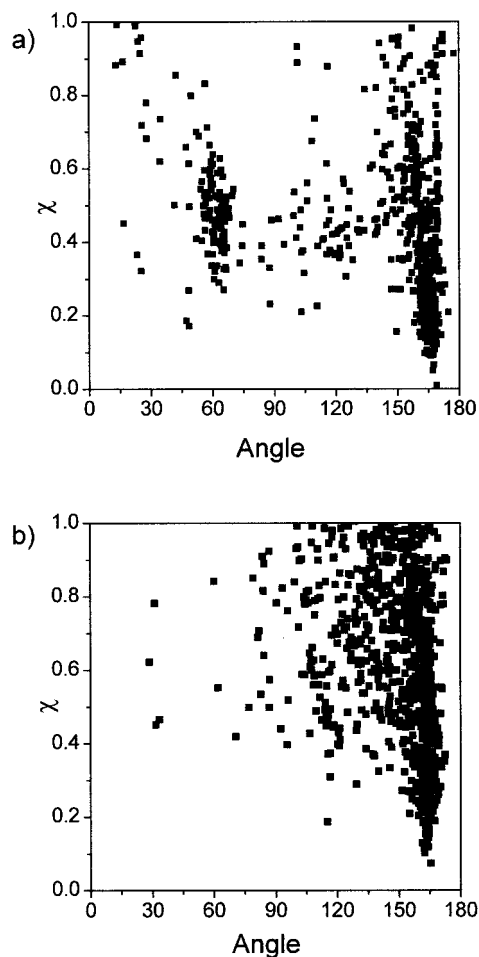


FIGURE 6 χ as function of the angle formed between perpendicular vectors to fucose and galactose ring planes (see text for definition). (a) Le^x and (b) Le^a. The conformations are the same plotted in Figures 4 and 5 taken from the second Monte Carlo method.

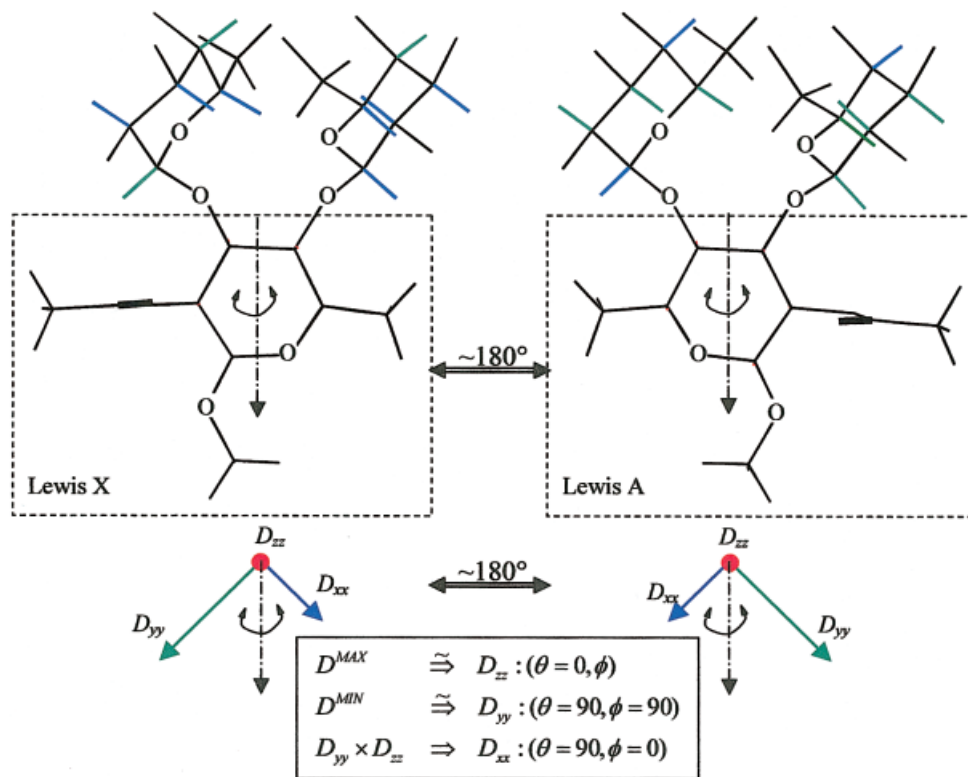


FIGURE 7 Model structures for Le^x and Le^a along with the principal axis directions of the respective orientational tensor. C—H bonds and the principal axis are color coded to explain the change in sign of the dipolar coupling values by symmetry relation (see text).

the broken line arrow. Apparently the orientation tensors for Le^a and Le^x are related by just such a rotation (Figure 7), which leaves the $^1D_{\text{CH}}$ for the GlcNAc residue unchanged but transforms all the positive dipole coupling values of the Fuc and Gal residues (blue, approximately parallel to the D_{xx} axis) into negative ones (green, approximately parallel to the D_{yy} axis) and vice versa.

CONCLUSION

We have presented here structural studies of oligosaccharides based on $^1D_{\text{CH}}$ experimental data combined with molecular modeling. For oligosaccharides of two or more residues exhibiting internal motions of the first kind,¹³ the measurement of five or more residual dipolar couplings corresponding to nonparallel C—H vectors makes it possible to derive accurate model structures from these data alone. As model cases the trisaccharides Le^x and Le^a β -methyl glycosides were studied in partially oriented liquid crystal solutions. We developed a strategy for rapid calculation of the difference between theoretical and experimental dipolar couplings for thousands of model structures gen-

erated by computer simulations, from which we obtain an accurate model reproducing the experimental values. In this way the theoretical model is “compared” with the actual structure through the $^1D_{\text{CH}}$ by using the merit function.

In this work we use simple molecular modeling principally as a source of model structures to search for the best fit to the experimental data. Two Monte Carlo strategies were explored in an attempt to guarantee both completeness and accuracy. In the first, several thousands of high energy structures were generated by screening the largest angular space possible. In the second, a protocol is implemented to obtain a greater number of structures in regions of lower energy. A rapid two-stage algorithm to evaluate the suitability of these structures for reproducing the dipolar coupling data was implemented. The first stage consisted of a comprehensive grid search followed by an intensive use of the Powell algorithm for optimizing the best initial orientations including experimental errors in the calculations in a last step. While the lowest value of the merit function corresponds to the best model, it is very informative to plot the dihedral angles in dipolar maps as a function of ϕ and ψ coded by the merit values. If the number of structures is

adequate, any inconsistency will be apparent. Plots of the energies of the models are also useful to verify the approximate agreement of the two calculations. A failure in agreement between the best structures obtained from $^1D_{CH}$ values and low energy conformations is an indication that the group of sugar residues does not have internal motion of the first kind, and may be exhibiting conformational exchange between two or more substantially different conformers. Such internal motion of the second kind requires a different strategy for analysis.^{9,14}

REFERENCES

1. Feizi, T. *Trends Biochem Sci* 1991, 16, 84–86.
2. Miller, K. E.; Mukhopadhyay, C.; Cagas, P.; Bush, C. A. *Biochemistry* 1992, 31, 6703–6709.
3. Xu, Q.; Bush, C. A. *Biochemistry* 1996, 35, 14521–14529.
4. Poveda, A.; Jiménez-Barbero, J. *Chem Soc Rev* 1998, 27, 133–143.
5. Jiménez-Barbero, J.; Asensio, J. L.; Cañada, F. J.; Poveda, A. *Curr Opin Struct Biol* 1999, 9, 549–555.
6. Imberty, A. *Curr Opin Struct Biol* 1997, 7, 617–623.
7. Martín-Pastor, M.; Bush, C. A. *Biochemistry* 2000, 39, 4674–4683.
8. Martín-Pastor, M.; Bush, C. A. *Carbohydr Res* 2000, 323, 147–145.
9. Martín-Pastor, M.; Bush, C. A. *J Biomol NMR* 2001, 19, 125–139.
10. Kiddle, G. R.; Homans, S. W. *FEBS Lett* 1998, 436, 128–130.
11. Rundlëf, T.; Landersjö, C.; Lycknert, K.; Maliniak, A.; Widmalm, G. *Magn Reson Chem* 1998, 36, 773–776.
12. Bolon, P. J.; Al-Hashimi, H. M.; J. L.; Prestegard, J. H. *J Mol Biol* 1999, 293, 107–115.
13. Martín-Pastor, M.; Bush, C. A. *Biochemistry* 1999, 38, 8045–8055.
14. Tian, F.; Al-Hashimi, H. M.; Craighead, J. L.; Prestegard, J. H. *J Am Chem Soc* 2001, 123, 485–492.
15. Mukhopadhyay, C.; Bush, C. A. *Biopolymers* 1991, 31, 1737–1746.
16. Imberty, A.; Mikros, E.; Koca, J.; Mollicone, R.; Oriol, R.; Pérez, S. *Glycoconj J* 1995, 12, 331–349.
17. Kogelberg, H.; Rutherford, T. J. *Glycobiology* 1994, 4, 49–57.
18. John, B. K.; Plant, D.; Hurd, J. B. *J Magn Reson Ser A* 1992, 101, 113–117.
19. Mohamadi, F.; Richards, N. G. J.; Guida, W. C.; Liskamp, R.; Lipton, M.; Caufield, C.; Chang, G.; Hendrickson, T.; Still, W. C. *J Comput Chem* 1990, 11, 440.
20. Allinger, N. L.; Yuh, Y. H.; Lii, J.-H. *J Am Chem Soc* 1989, 111, 8551.
21. Still, W. C.; Tempczyk, A.; Hawley, R. C.; Hendrickson, T. *J Am Chem Soc* 1990, 112, 6127.
22. Parrill, A. L.; Mamuya, N.; Dolata, D. P.; Gervay, J. *Glycoconj J* 1997, 14, 523–529.
23. Woods, R. J. *Glycoconj J* 1998, 15, 209–216.
24. Tjandra, N.; Bax, A. *Science* 1997, 278, 1111–1114.
25. Clore, G. M.; Gronenborn, A. M.; Bax, A. *J Magn Reson* 1998, 133, 216–221.
26. Emsley, J. W. In *Encyclopedia of Nuclear Magnetic Resonance*; Grant, D. M., Harris, R. K., Eds.; Wiley: Chichester, 1996 ; pp 2788–2799.
27. Lipari, G.; Szabo, A. *J Am Chem Soc* 1982, 104, 4546–4559.
28. Tjandra, N.; Grzesiek, S.; Bax, A. *J Am Chem Soc* 1996, 118, 6264–6272.
29. Thogersen, H.; Lemieux, R. U.; Bock, K.; Meyer, B. *Can J Chem* 1982, 60, 44–57.
30. Ichikawa, Y.; Lin, Y.-C.; Dumas, D. P.; Shen, G.-J.; García-Junceda, E.; Williams, M. A.; Bayer, R.; Ketcham, C.; Walker, L. E.; Paulson, J. C.; Wong, C.-H. *J Am Chem Soc* 1992, 114, 9283–9298.
31. Homans, S.; Forster, M. *Glycobiology* 1992, 2, 143–151.
32. Pérez, S.; Mouhous-Riou, N.; Nifant'ev, N. E.; Tsvetkov, Y. E.; Bachet, B.; Imberty, A. *Glycobiology* 1996, 6, 537–542.
33. Cagas, P.; Bush, C. A. *Biopolymers* 1990, 30, 1123–1138.